IRIS AperTO

UNIVERSITÀ DEGLI STUDI DI TORINO

AperTO - Archivio Istituzionale Open Access dell'Università di Torino

Higher metastatic efficiency of KRas G12V than KRas G13D in a colorectal cancer model

This is a pre print version of the following article:

Original Citation:

Availability:

This version is available http://hdl.handle.net/2318/1506903 since 2016-03-25T11:00:42Z

Published version:

DOI:10.1096/fj.14-262303

Terms of use:

Open Access

Anyone can freely access the full text of works made available as "Open Access". Works made available under a Creative Commons license can be used according to the terms and conditions of said license. Use of all other works requires consent of the right holder (author or publisher) if not exempted from copyright protection by the applicable law.

(Article begins on next page)

02 May 2026

UNIVERSITÀ DEGLI STUDI DI TORINO

This is an author version of the contribution published on:

Alamo P,Gallardo A,Di Nicolantonio F,Pavon MA,Casanova I,Trias M,Mangues MA,Lopez-Pousa A,Villaverde A,Vazquez E,Bardelli A,Cespedes MV,Mangues R

Higher metastatic efficiency of KRas G12V than KRas G13D in a colorectal cancer model.

FASEB JOURNAL (2014)
DOI: 10.1096/fj.14-262303

The definitive version is available at:
http://www.fasebj.org/cgi/doi/10.1096/fj.14-262303

Title: Higher metastatic efficiency of KRas G12V than KRas G13D in a colorectal cancer model

Authors (p.o): Alamo P (1)(2), Gallardo A (2)(3), Di Nicolantonio Federica (4,5), Pavón MA (1)(2), Casanova I (1)(2), Trias M (2)(6), Mangues MA (7), Lopez-Pousa A (8), Villaverde A (2)(9), Vázquez E (2)(9), Bardelli A (4,5,10), Céspedes MV (1)(2)* and Mangues R*, ** (1)(2)

Author´s Affiliations: (1) Oncogenesis and Antitumor Drug Group, Biomedical Research Institute Sant Pau (IIB-SantPau), Hospital de la Santa Creu i Sant Pau, c/ Sant Antoni Maria Claret, 167, 08025 Barcelona, Spain; (2) CIBER de Bioingeniería, Biomateriales y Nanomedicina (CIBER-BBN), Barcelona, Spain; (3) Department of Pathology, Clínica Girona, C/ Joan Maragall, 26, 17002, Girona, Spain; (4) University of Torino, Department of Oncology, Str prov 142 Km 3.95, 10060 Candiolo, Torino, Italy. (5) Candiolo Cancer Institute – FPO, IRCCS, Str prov 142 Km 3.95, 10060 Candiolo, Torino, Italy. (6) Department of General and Digestive Surgery, Hospital de la Santa Creu i Sant Pau, 08025 Barcelona, Spain; (7) Department of Pharmacy, Hospital de la Santa Creu i Sant Pau, 08025 Barcelona, Spain; (8) Department of Medical Oncology, Hospital de la Santa Creu i Sant Pau, 08025 Barcelona, Spain; (9) Institut de Biotecnologia i de Biomedicina, Universitat Autònoma de Barcelona and Department de Genètica i de Microbiologia, Universitat Autònoma de Barcelona, Bellaterra, 08193 Barcelona, Spain (10) FIRC Institute of Molecular Oncology (IFOM), 20139 Milano, Italy

Author´s e-mails: Alamo P [palamo@santpau.cat]; Gallardo A [aga5962@comg.cat]; Di Nicolantonio Federica [federica.dinicolantonio@unito.it]; Pavón MA [mpavon@santpau.cat]; Casanova I [icasanova@santpau.cat]; Lopez-Pousa A, [alopezp@santpau.cat]; Trias M [mtrias@santpau.cat]; Mangues MA [mmangues@santpau.cat]; Vázquez E [esther.vazquez@uab.cat]; Villaverde A [antoni.villaverde@uab.cat]; Bardelli Alberto [alberto.bardelli@unito.it] Céspedes MV [mcespedes@santpau.cat]; Mangues R [rmangues@santpau.cat]

* RM and MVC contributed equally to this study

**** Corresponding author:** Ramon Mangues; Biomedical Research Institute Sant Pau (IIB-SantPau), Hospital de la Santa Creu i Sant Pau and CIBER (CIBER-BBN). c/ Sant Antoni Maria Claret, 167, 08025 Barcelona, Spain. Phone: +34 93 553 79 18; Fax: +34 93 553 78 72 rmangues@santpau.cat

Running title: KRas G12V is more metastatic than KRas G13D

Authors declare no conflicts of interest

F. Di Nicolantonio and A. Bardelli are co-inventors on a patent describing the process of making isogenic cell lines. A. Bardelli is a shareholder of Horizon Discovery, a company exploiting AAV-mediated genome editing to create isogenic cell lines, and to which the SW48 cells described in this study have been licensed for commercial use.

ABBREVIATIONS

Angpt2: angiopoietin 2

AAV: deno-associated-virus

CRC: colorectal cancer

CXCR4: C-X-C chemokine receptor type 4

DMEM: Dulbecco's Modified Eagle Medium

EGFR: Epidermal growth factor receptor

EMT: epithelial-mesenchymal transition

ERK: extracellular-signal-regulated kinases

FBS: fetal bovine serum

FFPE: formalin-fixed paraffin-embeded

H&E: Hematoxylin and eosin stain

ICH: immunohistochemistry

KRAS: Kirsten rat sarcoma viral oncogene homolog

KRas: protein that in humans is encoded by the *KRas* gene

KRas G13D: Kirsten rat sarcoma viral oncogene homolog with Aspartic mutation at codon 13

KRas G12V: Kirsten rat sarcoma viral oncogene homolog with Valine mutation at codon 12

KRas WT: KRas wild type

p: p-value

PI3K: Phosphatidylinositol-4,5-bisphosphate 3-kinase

PTHLH: parathyroid hormone-like hormone

SDF1α: stromal cell-derived factor 1

UPA/UPAR: Urokinase-type plasminogen activator system

VEGFA: Vascular endothelial growth factor A

WT: wild-type

ABSTRACT

Although all KRas point mutants are considered to have a similar prognostic capacity, their transformation and tumorigenic capacities vary widely. We compared the metastatic efficiency of KRas G12V and KRas G13D oncogenes in an orthotopic colorectal cancer (CRC) model. Following subcutaneous preconditioning recombinant clones of the SW48 CRC cell line (Kras WT) expressing the KRas G12V or KRas G13D allele were icroinjected in the mouse cecum. The percentage of animals developing lymph node metastasis was higher in KRas G12V than in KRas G13D mice. Micro, macro and visible lymphatic foci were 1.5-3.0 fold larger in KRas G12V than in KRas G13D mice ($p<0.05$) . In lung, only microfoci were developed in both groups. KRas G12V primar tumors had lower apoptosis (7.0±1.2 vs 7.4±1.0 per field, $p=0.02$), higher tumor budding at the invasion front (1.2±0.2 vs. 0.6±0.1, $p=0.04$) and a higher percentage of CXCR4-overexpressing intravasated tumor emboli (49.8±9.4% vs. 12.8±4.4%, $p<0.001$) than KRas G13D tumors. KRas G12V primary tumors showed Akt activation, and β5 integrin, VEGF-A and Serpine-1 overexpression, whereas KRas G13D tumors showed integrin β1 and Angpt-2 oeverexpression. The increased cell survival, invasion, intravasation and specific molecular regulation observed in KRas G12V tumors is consistent with the higher aggressiveness observed in CRC patients expressing this oncogene.

Key words: KRas mutants, in vivo models aggressiveness

INTRODUCTION

The high incidence, poor prognosis and metastatic spread of colorectal cancer (CRC) makes this disease the second most common cause of cancer death in western countries. Forty percent of colorectal tumors bear mutations in the KRas gene, the most frequent being the substitution of Gly (KRas WT) by Val (KRas G12V), or Asp, at codon 12 and Gly by Asp at codon 13 (KRas G13D) (1). Most studies investigating the Kras oncogene as a prognostic marker do not differentiate between point mutants and assume all mutants have a similar impact on tumor biology. However, studies in CRC patients, in animal models and in vitro indicate otherwise.

In CRC, the first studies on the incidence of KRas mutations in codon 12 suggested that different mutations may have a different risk for tumor progression. They found that the prevalence of the different KRas oncoproteins varied among adenomas and among Dukes A, B and C tumors (2). The RASCAL study later established the KRas G12V mutation as the most aggressive KRAS mutation, associating it with a higher risk of recurrence and death in a large CRC patient cohort (3-5). This finding was later confirmed in a larger series (n=4,268) (3-5). Consistently, KRas G12V mutation confers a metastatic phenotype that renders CRC tumors more aggressive since the incidence of this mutation was found to be higher in primary tumors and metastases of Dukes C/D than in A/B primary tumors. Moreover, within the Dukes' D cases, KRas G12V mutations were associated with decreased overall survival (2, 6). Distinct Kras oncogene mutations have also shown different transformation capacity in 3T3 fibroblasts in vitro (2, 6). In another study it was seen that 3T3 transformants that express KRasG12C and KRas G13D show significant differences in their regulation of survival and anchorage-independent growth and in the induction of anoikis in culture (7). It has also been shown that these two transformants generate different sarcoma tumor types when injected in inmunosuppressed mice (8, 9).

The known differences in the transformation capacity in vitro and tumorigeneicity in vivo of different KRas point mutants led us to hypothesize that specific oncogenic KRAS changes, could also have different metastatic capacity. The main aim of this study was to compare the metastagenic capacity of two SW48 human CRC recombinant clones, expressing KRas G12V or KRas G13D mutants, after their subcutaneous preconditioining followed by orthotopic implantation in the cecum.

MATERIALS AND METHODS

SW48 KRas recombinant clones. The SW48 recombinants expressing heterozygous KRasVal12 (KRas G12V) or KRasAsp13 (KRas G13D) oncogenic mutation were generated by homologous recombination using an adeno-associated-virus (AAV), as previouly described (10). The mutations are knocked-in in a heterozygous fashion and the mutant allele are therefore expressed under the gene's own promoter. Clones obtained were sequenced to verify the presence of the corresponding KRas point mutation. SW48 control cells bearing the empty vector (KRas WT; KRas protooncogene) and the KRas G12V or KRas G13D recombinants clones were

cultured in DMEM (ref. 10829018, Invitrogen, UK) supplemented with 10% FBS (ref. F2442, Sigma-Aldrich, St Louis, USA), 50 units/ml penicillin and 50 mg/ml streptomycin (re. 15140122, Invitrogen).

Generation of the SW48 metastatic colorectal cancer models. We used five-week-old Swiss female nu/nu mice weighing 18 to 20 g (Charles River,L-Abreslle, France) for all in vivo experiments. Mice were housed in a sterile environment with bedding, water and γ-ray-sterilized food ad libitum. Experiments were approved by the Animal Ethics Committee at Hospital de la Santa Creu i Sant Pau.

In a preliminary study, we injected the SW48 recombinants expressing KRas G12V or KRas G13D directly into cecum. Due to the low metastatic rate we used subcutaneous preconditioning before orthotopic injection. This procedure was developed for colorectal cancer models that increase the metastatic rate without changing the pattern of metastases (11). This approach provided a sufficient rate of metastasis to compare metastatic development and regulation between KRas G12V- and KRas G13D-derived models.

Briefly, five mice were subcutaneously injected with $2x10^7$ control SW48 cells or $2x10^7$ recombinant cells (KRas G12V or KRas G13D) in DMEM, in two flanks. Tumors were excised when they reached a volume of 700 mm^3 and disaggregated. A cell suspension (2×10^6 cells re-suspended in 50 µl) derived from SC tumors was injected directly into the mouse cecum wall in control (KRas WT, n=9) and KRas G12V (n=11) and KRas G13D (n=7) mice using the orthotopic cell microinjection procedure (12). Mice were followed up once a week and sacrificed when had lost 10% of their body weight or showed signs of pain or illness.

Necropsy and histopatological analysis of primary tumor and metastases. At death, complete necropsy examination of each animal was performed. We recorded the presence and size of the primary tumor and any visible metastasic foci. Local tumor and the organs with expected metastases (lymph nodes, liver and lung) were removed, collected and processed for the histopathological analysis and molecular studies as described previously (12) .

Histopathology of primary tumor and all targeted metastatic organs was analyzed by two independent observers in stained H&E samples using 4x-20x magnification. We counted the number and area of micro- and macroscopic tumor foci in the affected organs using CellD Olympus software (v3.3). Foci with a diameter of 1mm or larger, occupying an area >750000 mm^2 (13) were considered macroscopic. All smaller foci were considered microscopic.

In primary tumors, we recorded the degree of differentiation and cell morphology, the percentage of tumor necrotic area, the apoptotic and mitotic rate, and the tumor invasion. The apoptotic rates were calculated by counting the number of apoptotic figures in ten ramdomly selected 400x field sections stained with HE. The primary tumor invasive capacity was analysed as previously described (11). Briefly, after anti-A1/A3 keratin staining, we counted the number of keratin positive single epithelial tumor cells as well as tumor cell clusters

containing ten or less cells (tumor budding) at the primary tumor front. We recorded the number of keratin positive cells or clusters in 3 different tumor fields (400x magnification) for each group.

Molecular analysis of primary tumors and metastatic foci. Molecular analysis was performed using immunohistochemistry (IHC) on formalin-fixed paraffin-embeded (FFPE) tumor tissue. IHC staining was performed using the DAKO Autostainer automated Link48 (Dako, California,USA) and standard procedures. Samples were incubated with the corresponding primary antibody using the following dilutions: integrin β1, β2, β3, β4, β5, α1, α2, α3, α4, α5, α6 and αv (1:100. Ref. ECM440. Chemicon, Atlanta, USA), AKT-p (1:10. Ref. M3628, Dako), ANGPT2 (1:50. Ref. AP10103b Abgent, San Diego, USA), MAPK-P (1:100. Ref. 4676, Cell Signaling, Danvers, MA, USA), P-MAPK-38 (1:100. Ref. 9211S, Cell signalling), Vimentin (1:300. Ref. M0725, Dako), PTHLH (1:50 Ref. ABIN394303, Abgent), VEGFA (1:1000. Ref. ab46154, Abcam, UK), beta-catenin (1:300. Ref. M33539, Dako), serpine1 (1:750. Ref ab28207. Abcam), CXCR4 (1:300, Abcam (clone UMB2; #3108-1)), anti-A1/A3 keratin (1:100. Ref. M7003, Dako), CD34 (ready to use, Ref. IR632, Dako), E-cadherin (1:400. Ref. 610182, BD Transduction Laboratories, New Yersey, USA), which were followed by incubation with mouse or rabbit secondary antibodies (EndVision, DAKO). We next incubated the preparation with DAB substrate (DAKO) for 5 min, and contrasted thiswith hematoxylin. Immuhistochemical slides were evaluated by two independent observers who quantified the percentage of stained cells in relation to the total number of tumor cells, and their staining intensity (between 0 and 3, where 3 represented the maximum intensity). Finally, the multiplication of both values represented the expression of the protein in each sample.

ELISA assays were performed to determine VEGF-A in primary tumor samples extracts following the manufacturer's recommendations (eBioscience Human VEGF-A Platinum ELISA, ref. BMS277/2CE for VEGFA).

Statistical analysis. Fisher's exact test was used to analyze possible significant differences between groups in primary tumor or metastasic rates. The Mann-Whitney test was used to compare tumor size, the number of apoptotic or mitotic figures, single tumor cells, and tumor clusters or metastatic foci between groups. Differences in survival between groups were evaluated using Kaplan-Meier curves and the Log-rank test. All quantitative values were expressed as mean±SE and the statistical tests were performed using SPSS version 11.0 (IBM, New York, USA). Differences between groups were considered significant at $p < 0.05$.

RESULTS

KRas G12V or KRas G13D expression yields higher metastatic rate and aggresiveness than wild type KRas .Mice bearing KRas G12V or KRas G13D onocogene expressing tumors had shorter survival than the KRas WT group (190±20 days, p=0.04 for KRas G12V, 188± 36 days for KRas G13D and 265±18 days for

KRas WT, $p< 0.001$). The take rate was 33% (3/9) in the KRas WT group, 73% (8/11) in the KRas G12V group and 57% (4/7) in the KRas G13D group. These differences were not significant (Table 1). Mean primary tumor volume at necropsy was significantly higher in both KRas G12V (1,201±83 mm^3, $p<0.05$) or the KRas G13D (1,395±118 mm^3, $p<0.01$) groups than in KRas WT mice (964±23 mm^3). Consequently, KRas mutants groups led to mouse death from intestinal obstruction earlier than in the KRas WT group. All groups developed undifferentiated stage IV tumors, with 40-70% necrosis and a high degree of vascular invasion.
Related to metastatic dissemination, all three groups developed lymphatic and lung metastases (Figure 1, Table 1), whereas no liver metastases were recorded in any group. The number of mice developing lymph node metastases was also higher in KRas G12V (73%) and KRas G13D (29%) than in KRas WT (11%) mice. Moreover, there was a significantly higher number of lymph node metastatic foci in KRas G12V (n=26) or KRas G13D (n=41) than in KRas WT mice ($p<0.05$). Similarly, the number of lung metastases in KRas G12V (n=34) and KRas G13D (n=27) was significantly higher than in KRas WT (n=10) mice (Table 1)

KRas G12V showed higher tumor cell survival, invasion and CXCR4 expressing intravasated tumor emboli than KRas G13D. We analyzed the number of apoptotic and mitotic cells in H&E sections derived from KRas G12V and KRas G13D primary tumors. KRas G12V primary tumors displayed a significantly ($p=0.02$) lower number of apoptotic figures per field (7.0± 1.2) than KRas G13D tumors (7.4±1.0) (Fig. 2A,B). Analysis of the mitotic rate showed a trend towards a higher number of mitotic figures in KRas G12V (4.9±0.5) than in KRas G13D (2.8±0.4) primary tumors but they did not reach statistical significance (not shown). In contrast to the observations in primary tumors, the mitotic and apoptotic parameters in KRas G12V and KRas G13D metastatic foci displayed no significant differences between groups (not shown).
We also analyzed the invasion front in the primary tumors. We counted the number of single tumor epithelial cells and the number of tumor buds (Figure 2C,D). The number of tumor buds (clusters of ten or fewer tumor cells) in the primary tumors (white arrows Fig. 2C) of the KRas G12V group was significantly ($p=0.04$) higher than the number of clusters (1.2±0.2/field) in the KRas G13D group (0.6±0.1/field) (Fig. 2D,G). In contrast, the number of single epithelial tumor cells at the invasion front was not significantly different between groups.

Based on the established relationship between the induction of epithelial mesenchymal transition (EMT) in tumor cells and the acquisition of an increased invasive and metastatic capacities (14), we studied the expression of Snail-1, as a molecular marker of EMT and the expression of E-cadherin (downregulated during EMT) and beta-catenin (upregulated during EMT) in the primary tumors, especially at their invasion front, of both groups. We found no differences in Snail-1, E cadherin and beta catenin expression between KRas G12V and KRas G13D groups (data not shown).

To assess differences in intravasation capacity and CXCR4 expression, we counted the number ot tumor emboli inside blood vessels in the tissues adjacent to the primary tumors (Figure 2) and performed a CXCR4 inmunostaining. We observed no significant differences in the number of intravasated tumor emboli in the

submucosal and pericolic layers of the cecum between groups. The percentage of tumor cells with CXCR4 membrane expression in intravasated tumor emboli of KRas G12V mice **(**49.8+9.4%) was significantly (*p<0.001*) higher than in KRas G13D **(**12.8+4.4%)intravasated tumor emboli (Figure 2E,F,H).

KRas G12V promotes a higher growth rate in lymph node metastases than KRas G13D mice. We analyzed the number of lymphatic and lung metastasis, determining their size and classified them into micro-, macro- and visible metastases. Regarding lymphatic metastasis, the percentage of affected mice was significantly higher in KRas G12V (73%, 8/11) than in KRas G13D (23%, 2/7) mice (Figure 1, Table 1). Moreover, in KRas G12V mice the mean area of lymphatic microfoci (30.3±8.3 x10^4um^2) was significantly (p=0.02) larger than in KRas G13D mice (12.1±2.8 x10^4µm^2). The mean area of the lymphatic macrofoci in KRas G12V mice (193.2±28.6x10^4µm^2) was also larger than in KRas G13D mice (158.5x10^4um^2). Similarly, the mean area of visible lymphatic metastases in KRas G12V mice (7,523±1,937 x10^4µm^2) was significantly (p=0.05) larger than in KRas G13D mice (2,622±400 x10^4µm^2) (Figure 1, Table 1). Thus, as compared to KRas GD13, the expression of the KRas G12V oncogene increased lymph node colonization and increased metastatic foci growth in lymph nodes by promoting the transition form micro- to macrometastases and from macro- to visible metastases. Regarding the development of lung metastasis, there were no significant differences in the number of affected mice between KRas G12V and KRas G13D groups. The analysis of metastatic size showed only micrometastasis in KRas G12V or KRas G13D mice. The total number of lung metastases in KRas G12V mice (n=34) was higher than in KRas G13D mice (n=27). The mean size of the lung microfoci was significantly (p<0.001) larger in KRas G13D (11.9±3.8 x10^4µm^2) than in KRas G12V mice (6.4±1.5 x10^4µm^2) (Table 1, Figure 1). No hepatic metastases were observed in SW48-derived KRas WT, KRas G12V or KRas G13D mice.

KRas G12V and KRas G13D induced different molecular changes in primary tumors. The differences in metastatic dissemination between the KRas G12V and KRas G13D groups triggered the analysis of the expression and/or activation of proteins involved in signalling downstream of KRas (PI3K and MAPK pathways) as well as regulators of survival, adhesion, invasion and metastatic dissemination to unveil some of the molecular changes that could underlie the observed differences in metastatic dissemination.

KRas G12V primary tumors showed a modestly (p=0.05) higher activation of PI3K pathway than KRas G13D tumors (Figure 3) measured by the level of phospho-AKT. Nevertheless, in lymphatic and lung metastasis, there were no significant differences in AKT activation between the KRas G12V and KRas G13D groups. The activation of the Erk pathway, as measured by p-MAPK, showed a trend towards a higher activation in KRas G12V versus KRas G13D tumors (data not shown). No significant differences were recorded in the activation of the Erk pathway in lymph node or lung metastasis between KRas G12V and KRas G13D groups (data not shown).

To analyze whether the KRas G12V and KRas G13D oncogenes differentially regulated adhesion, we evaluated the expression of α (1, 2, 3, 4, 5, 6 and ν) and β (1, 2, 3, 4, 5 and 6) integrins by IHC. Of the 13 evaluated

integrins, only β5 and β1 showed a differential expression pattern between groups. The level of β1 integrin expression was significantly (p=0.039) higher in KRas G13D primary tumors than in KRas G12V tumors (Figure 4A,B). In contrast, the expression of β5 integrin was higher in the KRas G12V primary tumor than in KRas G13D tumors (p = 0.037, Figure 4G,H). In addition, the level of β5 or β1 integrin expression was low in both lymph node and lung metastases in the KRas G12V and KRas G13D groups. We did not therefore detect significant differences in the expression of these integrins in metastases between groups (Figure 4C-F, 4I-L).

We did not observe expression of CXCR4 in the bulk of primary tumors or their invasive front in KRas G12V and KRas G13D groups. However CXCR4 was expressed in a subset of cells in metastatic foci involving the lymph nodes, or lung metastasis. The percentage of tumor cells that overexpressed CXCR4 in their membrane in the metastases affecting the lymph nodes in KRas G12V mice was significantly (p=0.009) higher than that in KRas G13D mice (Figure 5). There were no significant differences between groups in CXCR4 expression in lung metastases. We also evaluated the expression of Serpine-1, a regulator of adhesion and invasion. The expression of Serpine-1, as measured by IHC, was significantly (p=0.033) higher in KRas G12V than in KRas G13D primary tumors. These differences in expression were not maintained at the metastatic sites. Thus, no significant differences in Serpine-1 expression in lymphatic metastases were found between KRas G12V and KRas G13D groups. In contrast, the expression of Serpine-1 in lung metastases was significantly (p<0.001) higher in KRas G13D than in KRas G12V mice (Figure 5).

In primary tumors, the expression of VEGFA measured by ELISA, showed significantly higher (p=0.025) levels in KRas G12V than in KRas G13D. We also used immunohistochemistry to detect VEGF-A expression in metastatic foci. We observed no significant differences in lymphatic metastatic foci between groups. In contrast, lung metastases in the KRas G13D group showed a significantly (p<0.001) higher level of VEGF-A expression in KRas G13D than in KRas G12V lung metastases (Figure 6). Angiopoietin-2 (Angpt2) is involved in angiogenesis and metastatic spread. The analysis of its expression by IHC showed that Angpt2 was significantly (p=0.022) higher in KRas G13D than in KRas G12V primary tumors. The observed differences in Angpt2 expression were also maintained in metastases, since KRas G13D displayed a significantly higher level of this protein in metastatic foci involving lymph nodes (p=0.048) and the lung (p <0.001) than in the KRas G12V group. The level of Angpt2 expression in lymph node metastases that developed in the KRas G13D group was significantly higher (p=0.045) than that observed in KRas G13D primary tumors (Figure 6).

Subcutaneous SW48 KRas G12V or SW48 KRas G13D tumors used to generate the metastatic orthotopic model mostly exhibited protein expression levels simlar to those found in the derived primary tumors (data not shown). These expression profiles differed from those that we were able to obtain from cell recombinants cultured in vitro. Therefore, most molecular changes appear to be induced during their subcutaneous passage.

DISCUSSION

KRas G12V enhances metastases to lymph nodes, an indication of its higher aggresiveness. Our aim was to evaluate whether there were differences in metastatic dissemination between SW48-derived mouse CRC models expressing the KRas G12V or the KRas G13D oncogene. We observed that the KRas G12V mutation increased the percentage of mice with lymph node metastases and also the area of lymphatic microfoci, macrofoci and visible lymph node metastases, as compared to KRas G13D. Therefore, the KRas G12V oncogene increased both the colonization of the lymph nodes and the growth rate of the metastatic foci at this site, promoting the transition from microfoci to large metastases. Our observation of the significantly higher capacity for KRas G12V expressing tumor cells to develop lymphatic metastases suggests higher tumor aggresiveness for this mutation. This argument is consistent with the presence of lymph node metastasis as the strongest predictor of poor prognosis in CRC patients (15). Moreover, the higher agressiveness observed in KRas G12V mice is consistent with the shorter overall survival observed in CRC patients with KRas G12V mutation compared to other Kras mutations, in the RASCAL study (3). In human CRC tumors, of twelve different point mutations found at KRas codon 12 or 13, only the KRas G12V mutation conveyed an increased risk of recurrence and death (3, 4). In another study, an analysis restricted only to Dukes' D patients showed that KRas G12V decreased overall survival as compared to other KRas mutations (6). In our study, we did not detect any difference between KRas G12V and KRas G13D mice regarding the percentage of animals with lung metastases. KRas G13D seems to stimulate the growth of the lung metastasis more than KRas G12V, but it does not appear to be able to induce the transition from micro- to macro-metastases, since all metastases remained microscopic both in KRas G13D and KRas G12V mice. In liver, we did not observe any metastatic dissemination, because the SW48 CRC cell line does not show an intrinsic ability to metastasize to the liver. We used the SW48 CRC cells because they bear the Kras wild type as well as because they have previously been reported to be amenable to genetic engineering by homologous recombination.

KRas G12V alters protein regulation and induces higher tumor cell survival, invasion and intravasation. KRas G12V and KRas G13D tumors presented differences in protein expressions involved in invasion, cell survival and intravasation processes. KRas G12V enhanced cell survival, invasion and intravasation and overexpressed CXCR4, β5 integrin, VEGF-A and Serpine-1, and overactivated Akt in primary tumors. These alterations may underlie the increased metastatic growth in the lymph nodes found in KRas G12V mice, as compared to KRas G13D. In agreement, the different ras mutants show markedly different transformation capacities (16, 17) and have been associated with different interaction with the downstream effectors (18). In our model, KRas G12V induced activation of the AKT pathway and showed a lower number of apoptotic markers in comparison to KRas G13D. It has been shown that the Ras Val12 oncogene activates the PI3K/Akt pathway (19, 20), whereas tumors use PKB/Akt pathway activation to inhibit apoptosis, leading to higher

migratory, invasive and metastatic capacities (21, 22). Consistently, we previously showed that the KRas G13D oncogene displays lower transformation capacity in fibroblasts , associated with Akt inactivation and increased apoptosis in vitro (7) and in vivo (8). Consequently, the KRas G13D oncogene yielded more indolent sarcomas than fibroblasts tranformed with the KRas Cystine 12 (KRas G12C), the expression of which was associated with Akt activation and less apoptosis. The activation of the Akt pathway has also been observed in stage II CRC patients where AKT activation predicts tumor recurrence (23).

We also observed that KRas G12V enhanced budding in primary tumors associated with enhanced lymph node metastases. In agreement with this finding, in CRC patients, tumor budding at the invasive front is associated with lymph node metastases and poor prognosis (24-28).

The increase of invasion observed in KRAS mutant tumors could be caused by several distinct molecular mechanisms. We discarded epithelial-mesenchymal transition (EMT) as responsible for the enhanced metastases observed in KRas G12V since we did not observe differences in single cell count, or in Snail-1, E-cadherin or β-catenin expression between KRas G12V and KRas G13D tumors at the invasive front, characteristic of EMT (14). Nevertheless, in CRC models, several reports support higher migratory and metastatic capacity for tumors that overexpress β5 integrin together with Akt activation (observed in our KRas G12V tumors) compared to tumors with β1 expression and Akt inactivation (observed in KRas G13D tumors). Similarly, migration of the SW480 CRC cell line (which expresses KRas G12V) in type I collagen is dependent on αvβ5 expression and Akt activation(29). In contrast, downregulation of αvβ5 integrin in this model leads to α2β1-dependent and Akt-independent migration, supporting a cross-regulation between β5 and β1 asosociated with differential Akt regulation(29). Moreover, αvβ5-dependent migration on vitronectin has been associated with enhanced liver metastases in the LM-LM6 CRC model, whereas Akt inactivation blocked this migration (30). Consistently, the KRas G12V oncogene mutation induces β5 expression and blocks integrin β1 expression in colon epithelial cells (31).

Serpine-1 is also overexpressed in KRas G12V tumors and may contribute to their enhanced invasiveness and metastases. Thus, in CRC patients, Serpine-1 overexpression in primary tumors is associated with lymph node metastasis (32), whereas high levels of Serpine-1 in plasma is a marker of poor prognosis (33). In addition, crosstalk between β5 and β1, like that described in CRC models, has been reported in fibroblasts, in which integrin β5 degradation leading to β1 upregulation is controlled by uPA/uPAR system activation (34). This system is inactivated by serpine-1-. This suggests that Serpine-1, a protein overexpressed together with β5 integrin in KRas G12V tumors, may regulate this crosstalk in our CRC model, when serpine-1 covalently binds to and inactivates the uPA/uPAR system.

In KRas G12V mice, we observed an increased percentage of CXCR4-overexpressing cells in intravasated tumor emboli in the submucosal and pericolic layers of the cecum. We also found also a higher number of CXCR4 cells in lymph node metastases. These findings suggest the CXCR4 receptor plays a role in intravasation, enhancing lymph node metastases in our model. This suggestion is in agreement with the

association between intravasated tumor emboli (35) and lymphovascular invasion (36) with lymph node metastasis and poor prognosis in CRC patients. Similarly, CXCR4 overexpression in primary tumors increased the risk of recurrence and poor survival (37) in CRC patients. Moreover, expression of CXCR4 in the HT29 CRC model favours tumor cell extravasation (38), whereas CXCR4 expression promotes the growth of CT-26 CRC micrometastases in the colonized organ (39). In addition, CXCR4+ HT29 CRC cells are capable of establishing a paracrine signaling with SDF1α secreting lymph node stromal cells (40) which may drive their dissemination towards this metastatic site. Similarly, CXCR4 expressing tumor cells are able to migrate through hypoxic SDF1α, secreting endothelial cells (transendothelial migration) and invade blood vessels in a breast cancer model (41).

In agreement with enhanced VEGF-A tumor expression and lymph node metastases observed in KRas G12V mice, VEGF-A and CXCR4 are associated with lymph node metastasis and poor prognosis in CRC patients (42-44). Similarly, in the CT26 CRC model, VEGF-A induces angiogenesis and promotes vascular permeability, leading to metastasic spread (45, 46). Finally, and in contrast with the reports on KRas G12V disregulated proteins, no publications on the prognostic value in CRC patients have been reported for the proteins overexpressed in KRas G13D tumors (integrin β1 or Angpt-2).

Differential protein regulation in KRas G12V and KRas G13D mice between primary tumors and metastases. Whereas protein expression in primary tumors may contribute to determine the mechanism of invasion and intravasation, such expression in metastases may indicate the pathway used for metastatic foci growth at the metastatic site. In our model, KRas G13D tumors overexpressed Angpt-2 and developed larger lung micrometastasis than with KRas G12V. In this regard, Angpt-2 expression in the primary tumor may have promoted colonization of the lung, because it enhances cancer cell extravasation by loosening the endothelial cell junctions, leading to increased metastasis in the lung (47, 48). In contrast, the high levels of Angpt2 observed in lung microfoci in KRas G13D mice may have determined the inability of these tumor cells to promote vacularization. It has been observed that high levels of Angpt-2 induce microvessel regression and tumor growth inhibition in the HT29 subcutaneous CRC model (49).

The oncogene expressed in primary tumors (KRas G12V or KRas G13D) may determine the pattern of protein expression. Interestingly, the pattern of protein expression we found in orthotopic primary tumors was already present in the subctutaneous tumors used for KRas G12V and KRas G13D preconditioning. Thus, both orthotopic and subcutaneous tumors that expressed KRas G12V showed higher Akt activation and integrin β5 overexpression than KRas G13D. However, the environment in the site where the tumor grows may also contribute to regulate protein expression in tumor cells. In contrast with our observations in primary tumors, the number of mitotic and apoptotic figures in KRas G12V and KRas G13D metastatic foci did not differ significantly between groups. Therefore, different metastatic organs appear to regulate apoptosis in a different way. We also observed that the pattern of protein expression in metastases differed greatly from the corresponding pattern in the primary tumor. This suggests that that the tumor environment also contributes to

determining this pattern. In support of this suggestion we observed that VEGF-A or Serpine-1 were overexpressed in KRas G12V but not in KRas G13D primary tumors. In lung metastases, these two proteins were overexpressed in KRas G13D compared to KRas G12V mice.

Clinical implications. In summary, this is the first report to describe a different metastatic capacity and a pattern of protein expression for distinct KRas point mutations in an orthotopic mouse CRC model, as well as an association between metastatic capacity and CXCR4-overexpressing tumor emboli. Our results have highlighted the need to consider the different KRas mutants as separate entities.

These results are consistent with the higher aggressivenes of KRas G12V mutant observed in CRC patients, as compared to any other KRas mutation and support the notion that different KRas mutants may associate with different prognosis. The different regulation of cell survival and Akt-p between KRas G12V and KRas G13D in our model may also indicate different responses between KRas G12V and KRas G13D to antitumor drugs. This is in agreement with the reported lack of Akt activation by KRas G13D (7, 8), and with the higher sensivity of KRas G13D CRC cells, as compared to KRas G12V, to the EGFR inhibitor cetuximab in vitro and longer overall survival in KRas G13D patients compared with other KRas mutations when being treated with the EGFR inhibitor cetuximab (50). However, more recent clinical data are contradictory (51) . Future studies should explore other KRas mutations with lower transforming capacity in relation to their ability to engage different pathway effectors, their their propensity to metastasize, as well as their impact on anticancer treatments.

ACKNOWLEDGEMENTS

We thank Carmen Cabrera for technical support and Carolyn Newey for revising the English text. We acknowledge performing animal work in the CIBER-BBN Nanotoxicology unit. R.M. acknowledges funding from Instituto de Salud Carlos III (grant PI12/01861), la Fundació La Marató de TV3 416/C/2013-2030 CIBER-BBN NanoMets project and AGAUR (2009-SGR1437).

AUTHOR CONTRIBUTIONS

PA designed and performed the experiments, analyzed the data and participated in text writing. AG carried out the histopathological analysis of mouse samples. FD performed the KRas homologous recombination experiments. IC and MAP performed the experiments and the statistical analyses of mice data. M.T and M.A.M analyzed data. EV, AV, FD and AB participated in the discussion of data and text writing. RM and MVC contributed equally to this study and they conceived the project, analyzed data, supervised the overall project, and wrote the manuscript.

REFERENCES

1. Barbacid, M. (1987) ras genes. *Annu Rev Biochem* **56**, 779-827
2. Moerkerk, P., Arends, J. W., van Driel, M., de Bruine, A., de Goeij, A., and ten Kate, J. (1994) Type and number of Ki-ras point mutations relate to stage of human colorectal cancer. *Cancer Res* **54**, 3376-3378
3. Andreyev, H. J., Norman, A. R., Cunningham, D., Oates, J. R., and Clarke, P. A. (1998) Kirsten ras mutations in patients with colorectal cancer: the multicenter "RASCAL" study. *J Natl Cancer Inst* **90**, 675-684
4. Andreyev, H. J., Norman, A. R., Cunningham, D., Oates, J., Dix, B. R., Iacopetta, B. J., Young, J., Walsh, T., Ward, R., Hawkins, N., Beranek, M., Jandik, P., Benamouzig, R., Jullian, E., Laurent-Puig, P., Olschwang, S., Muller, O., Hoffmann, I., Rabes, H. M., Zietz, C., Troungos, C., Valavanis, C., Yuen, S. T., Ho, J. W., Croke, C. T., O'Donoghue, D. P., Giaretti, W., Rapallo, A., Russo, A., Bazan, V., Tanaka, M., Omura, K., Azuma, T., Ohkusa, T., Fujimori, T., Ono, Y., Pauly, M., Faber, C., Glaesener, R., de Goeij, A. F., Arends, J. W., Andersen, S. N., Lovig, T., Breivik, J., Gaudernack, G., Clausen, O. P., De Angelis, P. D., Meling, G. I., Rognum, T. O., Smith, R., Goh, H. S., Font, A., Rosell, R., Sun, X. F., Zhang, H., Benhattar, J., Losi, L., Lee, J. Q., Wang, S. T., Clarke, P. A., Bell, S., Quirke, P., Bubb, V. J., Piris, J., Cruickshank, N. R., Morton, D., Fox, J. C., Al-Mulla, F., Lees, N., Hall, C. N., Snary, D., Wilkinson, K., Dillon, D., Costa, J., Pricolo, V. E., Finkelstein, S. D., Thebo, J. S., Senagore, A. J., Halter, S. A., Wadler, S., Malik, S., Krtolica, K., and Urosevic, N. (2001) Kirsten ras mutations in patients with colorectal cancer: the 'RASCAL II' study. *Br J Cancer* **85**, 692-696
5. Span, M., Moerkerk, P. T., De Goeij, A. F., and Arends, J. W. (1996) A detailed analysis of KRas point mutations in relation to tumor progression and survival in colorectal cancer patients. *Int J Cancer* **69**, 241-245
6. Al-Mulla, F., Going, J. J., Sowden, E. T., Winter, A., Pickford, I. R., and Birnie, G. D. (1998) Heterogeneity of mutant versus wild-type Ki-ras in primary and metastatic colorectal carcinomas, and association of codon-12 valine with early mortality. *J Pathol* **185**, 130-138
7. Guerrero, S., Casanova, I., Farre, L., Mazo, A., Capella, G., and Mangues, R. (2000) KRas codon 12 mutation induces higher level of resistance to apoptosis and predisposition to anchorage-independent growth than codon 13 mutation or proto-oncogene overexpression. *Cancer Res* **60**, 6750-6756
8. Guerrero, S., Figueras, A., Casanova, I., Farre, L., Lloveras, B., Capella, G., Trias, M., and Mangues, R. (2002) Codon 12 and codon 13 mutations at the KRas gene induce different soft tissue sarcoma types in nude mice. *FASEB J* **16**, 1642-1644
9. Cespedes, M. V., Casanova, I., Parreno, M., and Mangues, R. (2006) Mouse models in oncogenesis and cancer therapy. *Clin Transl Oncol* **8**, 318-329
10. Di Nicolantonio, F., Arena, S., Gallicchio, M., Zecchin, D., Martini, M., Flonta, S. E., Stella, G. M., Lamba, S., Cancelliere, C., Russo, M., Geuna, M., Appendino, G., Fantozzi, R., Medico, E., and Bardelli, A. (2008) Replacement of normal with mutant alleles in the genome of normal human cells unveils mutation-specific drug responses. *Proc Natl Acad Sci U S A* **105**, 20864-20869

11. Alamo, P., Gallardo, A., Pavon, M. A., Casanova, I., Trias, M., Mangues, M. A., Vazquez, E., Villaverde, A., Mangues, R., and Cespedes, M. V. Subcutaneous preconditioning increases invasion and metastatic dissemination in mouse colorectal cancer models. *Dis Model Mech* **7**, 387-396
12. Cespedes, M. V., Espina, C., Garcia-Cabezas, M. A., Trias, M., Boluda, A., Gomez del Pulgar, M. T., Sancho, F. J., Nistal, M., Lacal, J. C., and Mangues, R. (2007) Orthotopic microinjection of human colon cancer cells in nude mice induces tumor foci in all clinically relevant metastatic sites. *Am J Pathol* **170**, 1077-1085
13. Folkman, J. (1983) Angiogenesis: initiation and modulation. *Symp Fundam Cancer Res* **36**, 201-208
14. Alderton, G. K. (2013) Metastasis: Epithelial to mesenchymal and back again. *Nat Rev Cancer* **13**, 3
15. Resch, A., and Langner, C. (2013) Lymph node staging in colorectal cancer: old controversies and recent advances. *World J Gastroenterol* **19**, 8515-8526
16. Fasano, O., Aldrich, T., Tamanoi, F., Taparowsky, E., Furth, M., and Wigler, M. (1984) Analysis of the transforming potential of the human H-ras gene by random mutagenesis. *Proc Natl Acad Sci U S A* **81**, 4008-4012
17. Seeburg, P. H., Colby, W. W., Capon, D. J., Goeddel, D. V., and Levinson, A. D. (1984) Biological properties of human c-Ha-ras1 genes mutated at codon 12. *Nature* **312**, 71-75
18. Downward, J. (2003) Targeting RAS signalling pathways in cancer therapy. *Nat Rev Cancer* **3**, 11-22
19. Monaco, R., Chen, J. M., Friedman, F. K., Brandt-Rauf, P., Chung, D., and Pincus, M. R. (1995) Structural effects of the binding of GTP to the wild-type and oncogenic forms of the ras-gene-encoded p21 proteins. *J Protein Chem* **14**, 721-729
20. Pacold, M. E., Suire, S., Perisic, O., Lara-Gonzalez, S., Davis, C. T., Walker, E. H., Hawkins, P. T., Stephens, L., Eccleston, J. F., and Williams, R. L. (2000) Crystal structure and functional analysis of Ras binding to its effector phosphoinositide 3-kinase gamma. *Cell* **103**, 931-943
21. Vivanco, I., and Sawyers, C. L. (2002) The phosphatidylinositol 3-Kinase AKT pathway in human cancer. *Nat Rev Cancer* **2**, 489-501
22. Xue, G., and Hemmings, B. A. (2013) PKB/Akt-dependent regulation of cell motility. *J Natl Cancer Inst* **105**, 393-404
23. Malinowsky, K., Nitsche, U., Janssen, K. P., Bader, F. G., Spath, C., Drecoll, E., Keller, G., Hofler, H., Slotta-Huspenina, J., and Becker, K. F. Activation of the PI3K/AKT pathway correlates with prognosis in stage II colon cancer. *Br J Cancer* **110**, 2081-2089
24. Mitrovic, B., Schaeffer, D. F., Riddell, R. H., and Kirsch, R. (2012
) Tumor budding in colorectal carcinoma: time to take notice. *Mod Pathol* **25**, 1315-1325
25. Zlobec, I., Hadrich, M., Dawson, H., Koelzer, V. H., Borner, M., Mallaev, M., Schnuriger, B., Inderbitzin, D., and Lugli, A. (2014) Intratumoural budding (ITB) in preoperative biopsies predicts the presence of lymph node and distant metastases in colon and rectal cancer patients. *Br J Cancer* **110**, 1008-1013

26. Kazama, S., Watanabe, T., Ajioka, Y., Kanazawa, T., and Nagawa, H. (2006) Tumour budding at the deepest invasive margin correlates with lymph node metastasis in submucosal colorectal cancer detected by anticytokeratin antibody CAM5.2. *Br J Cancer* **94**, 293-298

27. Kye, B. H., Jung, J. H., Kim, H. J., Kang, S. G., Cho, H. M., and Kim, J. G. Tumor budding as a risk factor of lymph node metastasis in submucosal invasive T1 colorectal carcinoma: a retrospective study. *BMC Surg* **12**, 16

28. Giger, O. T., Comtesse, S. C., Lugli, A., Zlobec, I., and Kurrer, M. O. (2012) Intra-tumoral budding in preoperative biopsy specimens predicts lymph node and distant metastasis in patients with colorectal cancer. *Mod Pathol* **25**, 1048-1053

29. Defilles, C., Lissitzky, J. C., Montero, M. P., Andre, F., Prevot, C., Delamarre, E., Marrakchi, N., Luis, J., and Rigot, V. (2009) alphavbeta5/beta6 integrin suppression leads to a stimulation of alpha2beta1 dependent cell migration resistant to PI3K/Akt inhibition. *Exp Cell Res* **315**, 1840-1849

30. Yoshioka, T., Nishikawa, Y., Ito, R., Kawamata, M., Doi, Y., Yamamoto, Y., Yoshida, M., Omori, Y., Kotanagi, H., Masuko, T., and Enomoto, K. Significance of integrin alphavbeta5 and erbB3 in enhanced cell migration and liver metastasis of colon carcinomas stimulated by hepatocyte-derived heregulin. *Cancer Sci* **101**, 2011-2018

31. Yan, Z., Chen, M., Perucho, M., and Friedman, E. (1997) Oncogenic Ki-ras but not oncogenic Ha-ras blocks integrin beta1-chain maturation in colon epithelial cells. *J Biol Chem* **272**, 30928-30936

32. Sakakibara, T., Hibi, K., Koike, M., Fujiwara, M., Kodera, Y., Ito, K., and Nakao, A. (2005) Plasminogen activator inhibitor-1 as a potential marker for the malignancy of colorectal cancer. *Br J Cancer* **93**, 799-803

33. Nielsen, H. J., Pappot, H., Christensen, I. J., Brunner, N., Thorlacius-Ussing, O., Moesgaard, F., Dano, K., and Grondahl-Hansen, J. (1998) Association between plasma concentrations of plasminogen activator inhibitor-1 and survival in patients with colorectal cancer. *BMJ* **316**, 829-830

34. Huang, C.-C. L. a. T.-S. (2005) Plasminogen Activator Inhibitor-1: The Expression, Biological Functions, and Effects on Tumorigenesis
and Tumor Cell Adhesion and Migration *Journal of Cancer Molecules* **1**, 26-35

35. Son, H. J., Song, S. Y., Lee, W. Y., Yang, S. S., Park, S. H., Yang, M. H., Yoon, S. H., and Chun, H. K. (2008) Characteristics of early colorectal carcinoma with lymph node metastatic disease. *Hepatogastroenterology* **55**, 1293-1297

36. Lim, S. B., Yu, C. S., Jang, S. J., Kim, T. W., Kim, J. H., and Kim, J. C. (2010) Prognostic significance of lymphovascular invasion in sporadic colorectal cancer. *Dis Colon Rectum* **53**, 377-384

37. Kim, J., Takeuchi, H., Lam, S. T., Turner, R. R., Wang, H. J., Kuo, C., Foshag, L., Bilchik, A. J., and Hoon, D. S. (2005) Chemokine receptor CXCR4 expression in colorectal cancer patients increases the risk for recurrence and for poor survival. *J Clin Oncol* **23**, 2744-2753

38. Gassmann, P., Haier, J., Schluter, K., Domikowsky, B., Wendel, C., Wiesner, U., Kubitza, R., Engers, R., Schneider, S. W., Homey, B., and Muller, A. (2009) CXCR4 regulates the early extravasation of metastatic tumor cells in vivo. *Neoplasia* **11**, 651-661
39. Zeelenberg, I. S., Ruuls-Van Stalle, L., and Roos, E. (2003) The chemokine receptor CXCR4 is required for outgrowth of colon carcinoma micrometastases. *Cancer Res* **63**, 3833-3839
40. Margolin, D. A., Silinsky, J., Grimes, C., Spencer, N., Aycock, M., Green, H., Cordova, J., Davis, N. K., Driscoll, T., and Li, L. (2011) Lymph node stromal cells enhance drug-resistant colon cancer cell tumor formation through SDF-1alpha/CXCR4 paracrine signaling. *Neoplasia* **13**, 874-886
41. Jin, F., Brockmeier, U., Otterbach, F., and Metzen, E. (2013) New Insight into the SDF-1/CXCR4 Axis in a Breast Carcinoma Model: Hypoxia-Induced Endothelial SDF-1 and Tumor Cell CXCR4 Are Required for Tumor Cell Intravasation. *Mol Cancer Res* **10**, 1021-1031
42. Fukunaga, S., Maeda, K., Noda, E., Inoue, T., Wada, K., and Hirakawa, K. (2006) Association between expression of vascular endothelial growth factor C, chemokine receptor CXCR4 and lymph node metastasis in colorectal cancer. *Oncology* **71**, 204-211
43. George, M. L., Tutton, M. G., Janssen, F., Arnaout, A., Abulafi, A. M., Eccles, S. A., and Swift, R. I. (2001) VEGF-A, VEGF-C, and VEGF-D in colorectal cancer progression. *Neoplasia* **3**, 420-427
44. Ottaiano, A., Franco, R., Aiello Talamanca, A., Liguori, G., Tatangelo, F., Delrio, P., Nasti, G., Barletta, E., Facchini, G., Daniele, B., Di Blasi, A., Napolitano, M., Ierano, C., Calemma, R., Leonardi, E., Albino, V., De Angelis, V., Falanga, M., Boccia, V., Capuozzo, M., Parisi, V., Botti, G., Castello, G., Vincenzo Iaffaioli, R., and Scala, S. (2006) Overexpression of both CXC chemokine receptor 4 and vascular endothelial growth factor proteins predicts early distant relapse in stage II-III colorectal cancer patients. *Clin Cancer Res* **12**, 2795-2803
45. Criscuoli, M. L., Nguyen, M., and Eliceiri, B. P. (2005) Tumor metastasis but not tumor growth is dependent on Src-mediated vascular permeability. *Blood* **105**, 1508-1514
46. Weis, S., Cui, J., Barnes, L., and Cheresh, D. (2004) Endothelial barrier disruption by VEGF-mediated Src activity potentiates tumor cell extravasation and metastasis. *J Cell Biol* **167**, 223-229
47. Minami, T., Jiang, S., Schadler, K., Suehiro, J., Osawa, T., Oike, Y., Miura, M., Naito, M., Kodama, T., and Ryeom, S. (2013) The calcineurin-NFAT-angiopoietin-2 signaling axis in lung endothelium is critical for the establishment of lung metastases. *Cell Rep* **4**, 709-723
48. Rigamonti, N., and De Palma, M. A role for angiopoietin-2 in organ-specific metastasis. *Cell Rep* **4**, 621-623
49. Cao, Y., Sonveaux, P., Liu, S., Zhao, Y., Mi, J., Clary, B. M., Li, C. Y., Kontos, C. D., and Dewhirst, M. W. (2007) Systemic overexpression of angiopoietin-2 promotes tumor microvessel regression and inhibits angiogenesis and tumor growth. *Cancer Res* **67**, 3835-3844
50. De Roock, W., Jonker, D. J., Di Nicolantonio, F., Sartore-Bianchi, A., Tu, D., Siena, S., Lamba, S., Arena, S., Frattini, M., Piessevaux, H., Van Cutsem, E., O'Callaghan, C. J., Khambata-Ford, S., Zalcberg, J. R., Simes, J., Karapetis, C. S., Bardelli, A., and Tejpar, S. (2010) Association of KRAS

p.G13D mutation with outcome in patients with chemotherapy-refractory metastatic colorectal cancer treated with cetuximab. *JAMA* **304**, 1812-1820

51. Peeters, M., Douillard, J. Y., Van Cutsem, E., Siena, S., Zhang, K., Williams, R., and Wiezorek, J. Mutant KRAS codon 12 and 13 alleles in patients with metastatic colorectal cancer: assessment as prognostic and predictive biomarkers of response to panitumumab. *J Clin Oncol* **31**, 759-765

Table 1. Number and area of lymph nodes and pulmonary microfoci. macrofoci and visible metastases observed in KRas WT, KRas G12V and KRas G13D SW48 groups.

Metastatic Site	SW48 Group	Affected animales (n)	Metastatic dissemination* Micro		Macro		Visible	
			Foci (n)	Area mean± SE ($x10^5$ μm^2)	Foci (n)	Area mean± SE ($x10^5$ μm^2)	Foci (n)	Area mean± SE ($x10^5$ μm^2)
Lymph node	KRas WT	**1/9**[a]	0	**0**[c.d]	0	**0**[f.g]	2	2.486±1754
	KRas G12V	**8/11**[a.b]	12	**30.3±8.3**[e.c]	4	**193.2±28.6**[f]	10	**7.523 ±1937**[h]
	KRas G13D	**2/7**[b]	27	**12.1±2.8**[e.d]	1	**158.5** [g]	13	**2.622±400**[h]
Lung	KRas WT	**1/9**	**10**	**8.9±0.2**	0	0	0	0
	KRas G12V	**4/11**	**34**	**6.4±1.5**[i]	0	0	0	0
	KRas G13D	**2/7**	**27**	**11.9±3.8**[i]	0	0	0	0

n_f: *number foci*).

Statistical analysis: [a] *p= 0.03,* [b] *p=0.08 (Test de Fisher,.* [c] *p=0.05,* [d] *p=0.028,* [e] *p= 0.02,* [f,g] *p<0.001,* [h]*p=0.05,* [i]*p<0.001 (Mann Whitney Test)*

FIGURE LEGENDS

Figure 1. Primary tumor and metastasis development in KRas G12V and KRas G13D mouse models. No differences in primary tumor growth were observed between groups (A,B)**.** KRas G12V mice developed micro-, macro- and visible-metastasis in the lymph nodes (C), which were significantly bigger than the lymph node metastases that developed in KRas G13D mice (D). In contrast, KRasG12D and KRas G13D mice developed only microfoci in the lung; however, the lung microfoci in KRas G13D mice were significantly bigger (F) than in KRas G12V mice (E). The type of metastasis was established as a function of its diameter: microfoci <1mm; macrofoci 1-3 mm; visible >3mm; H&E staining. Original magnification: x40(C-F)

Figure 2. Reduced apoptosis and increased tumor budding and CXCR4-overexpressing intravasated emboli in KRas G12V primary tumors as compared to KRas G13D tumors. Primary tumors in KRas G12V mice (A, G) showed a significantly (p=0.019) lower number of apoptotic cells (white arrows) as compared to KRas G13D mice (B, G). In contrast, primary tumors in KRas G12V mice (C) showed a significantly (p=0.037) larger number of pan-keratin positive tumor clusters (budding) at the invasion front (black arrows), than KRas G13D mice (D, G). Intravasated tumor emboli in the submucosal and pericolic layers of the cecum had a significantly (p<0.001) higher percentage of cells overexpressing CXCR4 in KRas G12V (E,H) than in KRas G13D primary tumors (F,H). Count of apoptotic bodies, tumor emboli or tumor buds (clusters of 10 or fewer cells sourrounded by stroma at the invasive front) was performed in ten 400X magnified primary tumor fields. Original magnification : x400 (A-D); x200 (E-F)

Figure 3. KRas G12V primary tumors showed higher AKT activation than KRas G13D tumors. Primary tumors (A) in KRas G12V group showed a significantly (p<0.05) higher level of AKT activation than those (B) in the KRas G13D group. No differences in the activation of AKT in lymph node (C,D) or pulmonary (E,F) foci were observed between groups (E,F). Original magnification: x200 (A-F)

Figure 4. KRas G12V tumors overexpressed integrin β5, whereas KRas G13D tumors overexpressed integrin β1. Primary tumors (A) in KRas G12V group showed significantly lower β1 integrin expression than primary tumors (B) in the KRas G13D group. No expression of β1 integrin was detected in lymph node and pulmonary foci in any group (C-F). In contrast, primary tumors (G) in KRas G12V group showed significantly higher β5 integrin expression than primary tumous (H) in the KRas G13D group. No expression of β5 integrin was detected in lymph node or pulmonary foci in any group (I-L). Original magnification: x40(A-B); x200(C-L)

Figure 5. KRas G12V tumors higher levels of Serpine-1 in primary tumors, and of CXCR4 in lymph node metastasis, as compared to KRas G13D mice. Primary tumors in KRas G12V mice (A) showed significantly higher levels of Serpine-1 expression than primary tumors in KRas G13D mice (B). No differences in Serpine-1

expression in lymph node foci were observed between groups (C,D). In contrast, pulmonary foci in KRas G13D mice showed significantly higher expression of Serpine-1 than in KRas G12V mice (E,F). Primary tumors in KRAS G12V (G) or in KRas G13D (H) lacked CXCR4 expression. However, in lymph node metastases, KRas G12V mice showed significantly higher expression of CXCR4 in the membrane than KRas G13D mice (I,J). Low level of CXCR4 expression in pulmonary foci of KRas G12V (K) and KRas G13D (L) mice was observed, showing no significant differences between groups. Original magnification: x200(A-L)

Figure 6. KRas G12V tumors overexpressed VEGFA whereas KRas G13D tumors overexpressed Angpt2. Primary tumors in KRas G12V mice showed significant higher expression of VEGFA than in KRas G13D mice (A). In contrast, no differences in the VEGFA expression in lymph node foci were observed between groups (B,C); whereas in pulmonary foci the expression of VEGF-A was significantly lower in KRas G12V (D) than in KRas G13D (E) mice. KRas G12V primary tumors (F) showed significantly lower levels of Angpt2 expression than KRas G13D tumors (G). Similarly, lymph node (H,I) or pulmonary (J,K) metastasis in KRas G13D mice showed significantly higher Angpt2 expression than KRas G12V mice. Original magnification: x200(C-F); x100(G-L)

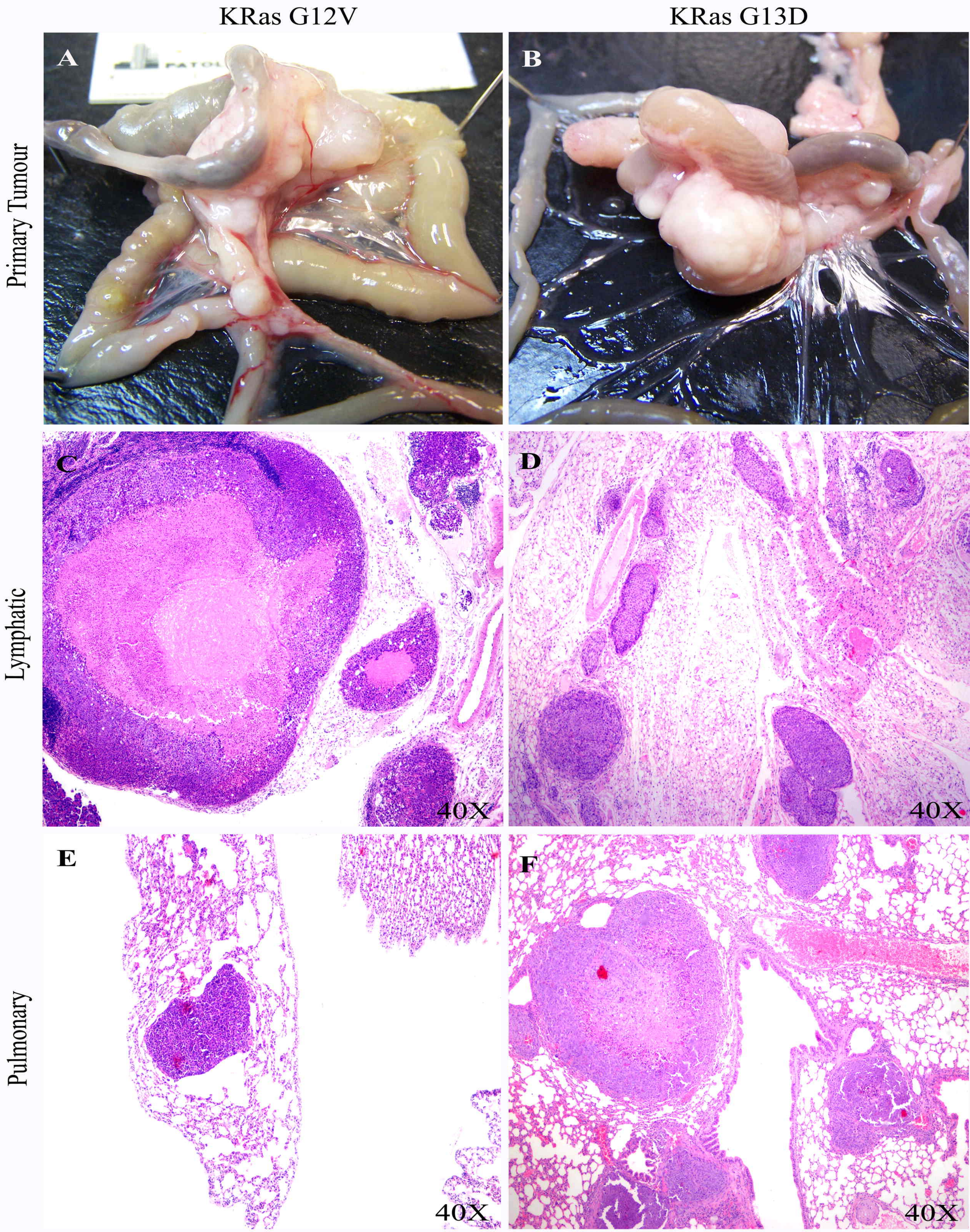
KRas G12V
KRas G13D
Primary Tumour
Lymphatic
Pulmonary
A
B
C
D
E
F
40X
40X
40X
40X

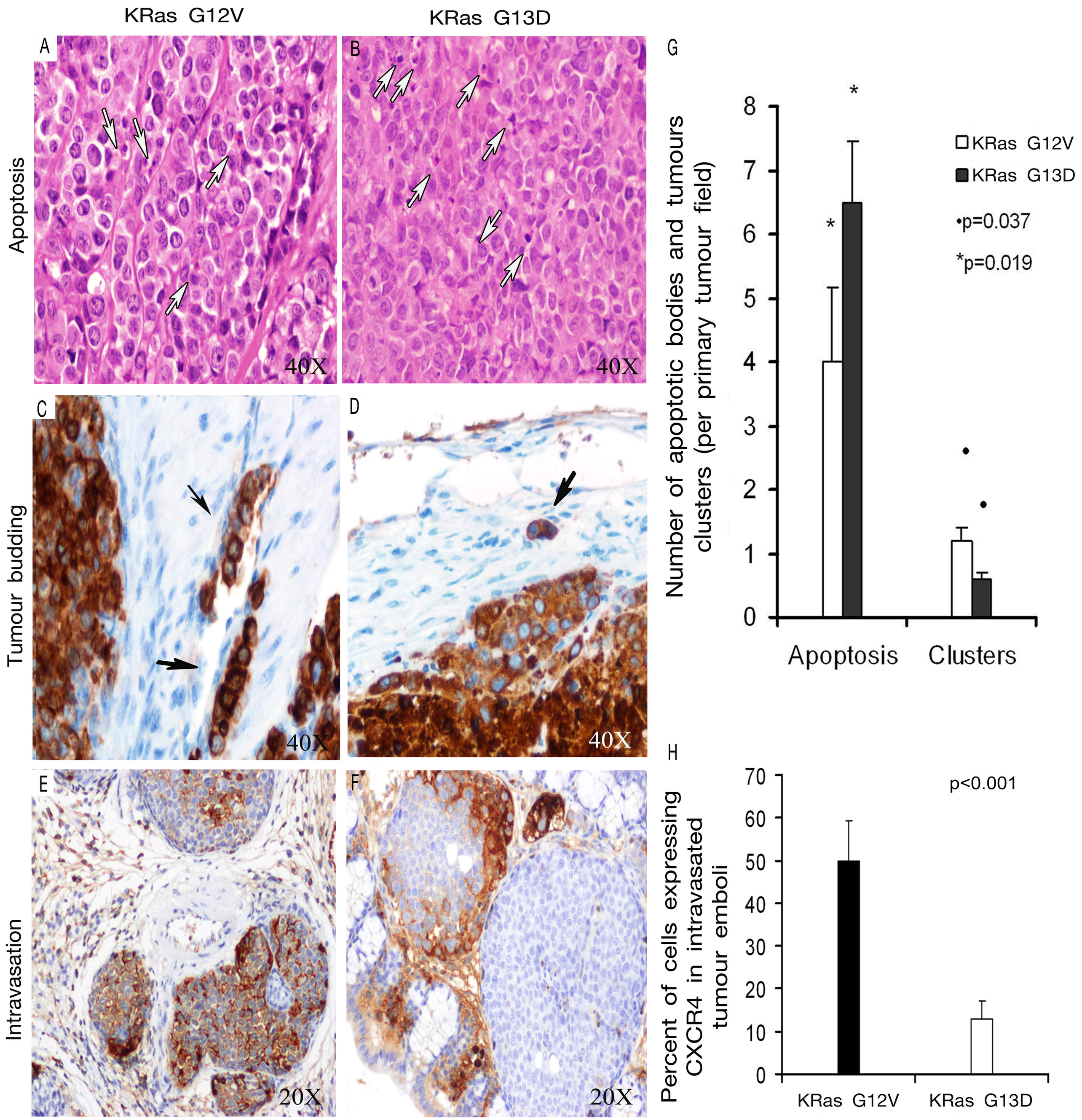
KRas G12V
KRas G13D
A
B
Apoptosis
40X
40X
C
D
Tumour budding
40X
40X
E
F
Intravasation
20X
20X
G
Number of apoptotic bodies and tumours clusters (per primary tumour field)
8
7
6
5
4
3
2
1
0
*
*
Apoptosis
Clusters
KRas G12V
KRas G13D
•p=0.037
*p=0.019
H
Percent of cells expressing CXCR4 in intravasated tumour emboli
70
60
50
40
30
20
10
0
p<0.001
KRas G12V
KRas G13D

Figure 2

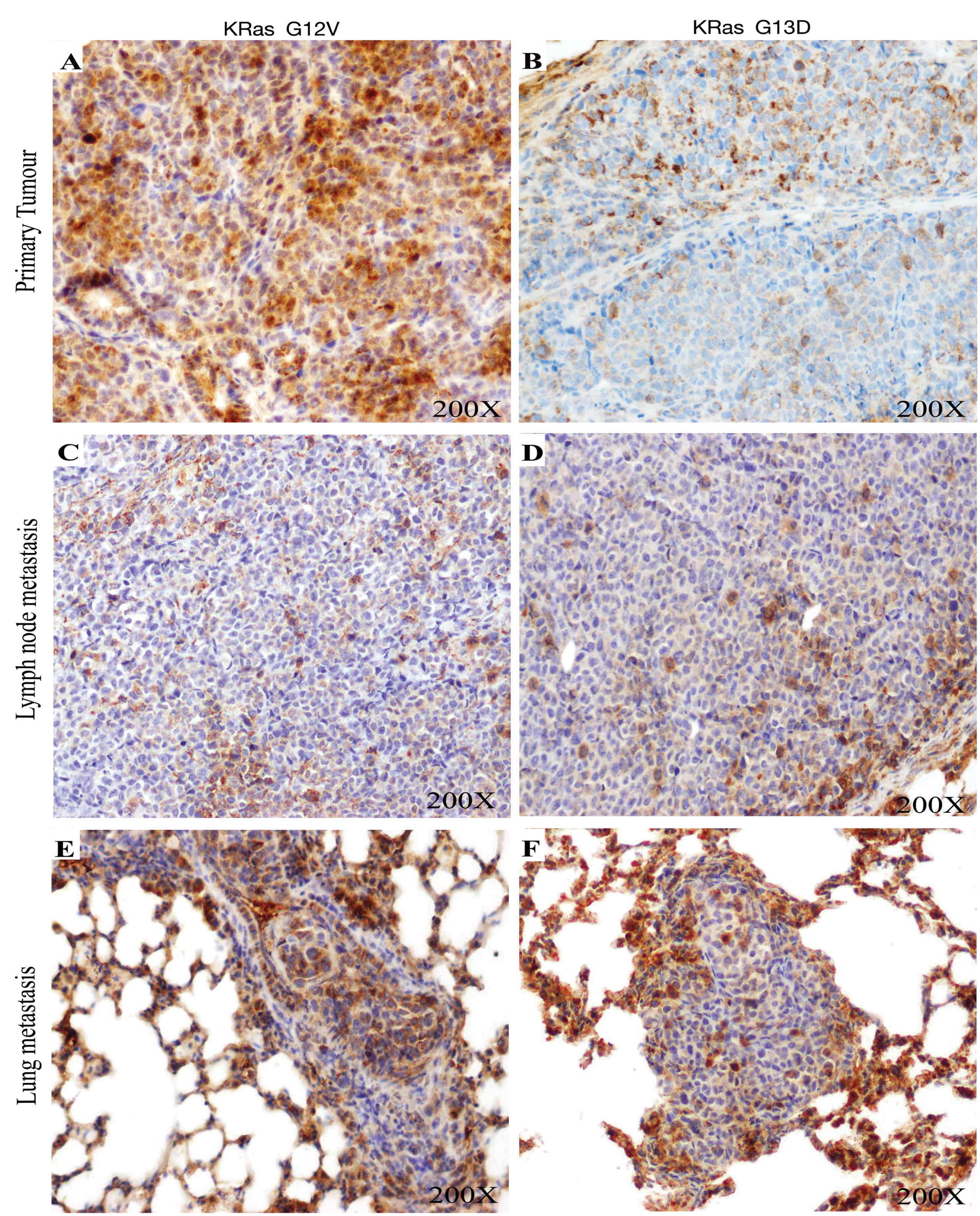
KRas G12V
KRas G13D
Primary Tumour
Lymph node metastasis
Lung metastasis
A
B
C
D
E
F
200X
200X
200X
200X
200X
200X

Figure 3

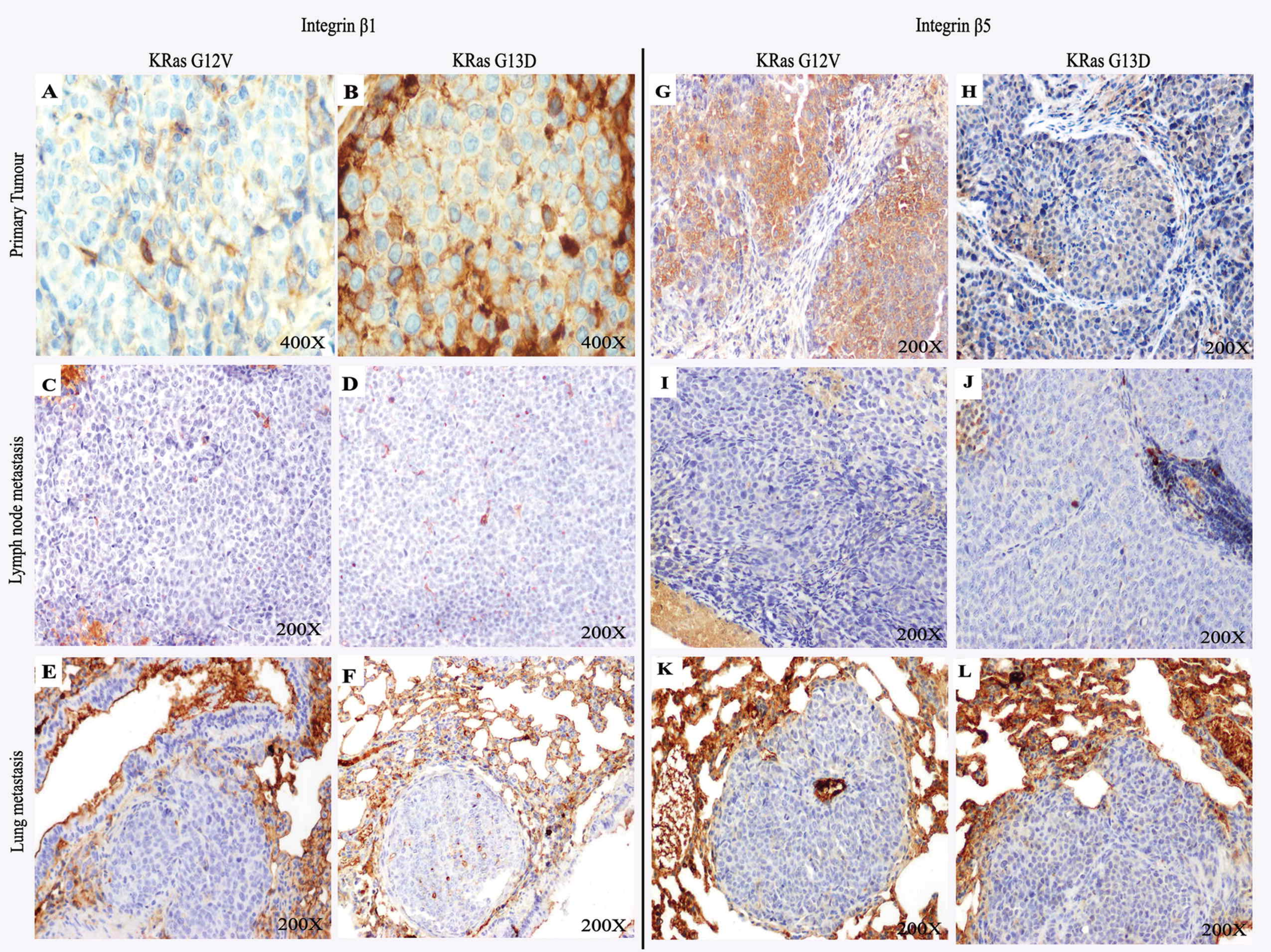
Integrin β1
Integrin β5
KRas G12V
KRas G13D
KRas G12V
KRas G13D
Primary Tumour
Lymph node metastasis
Lung metastasis
A
B
C
D
E
F
G
H
I
J
K
L
400X
400X
200X
200X
200X
200X
200X
200X
200X
200X
200X
200X

Figure 4

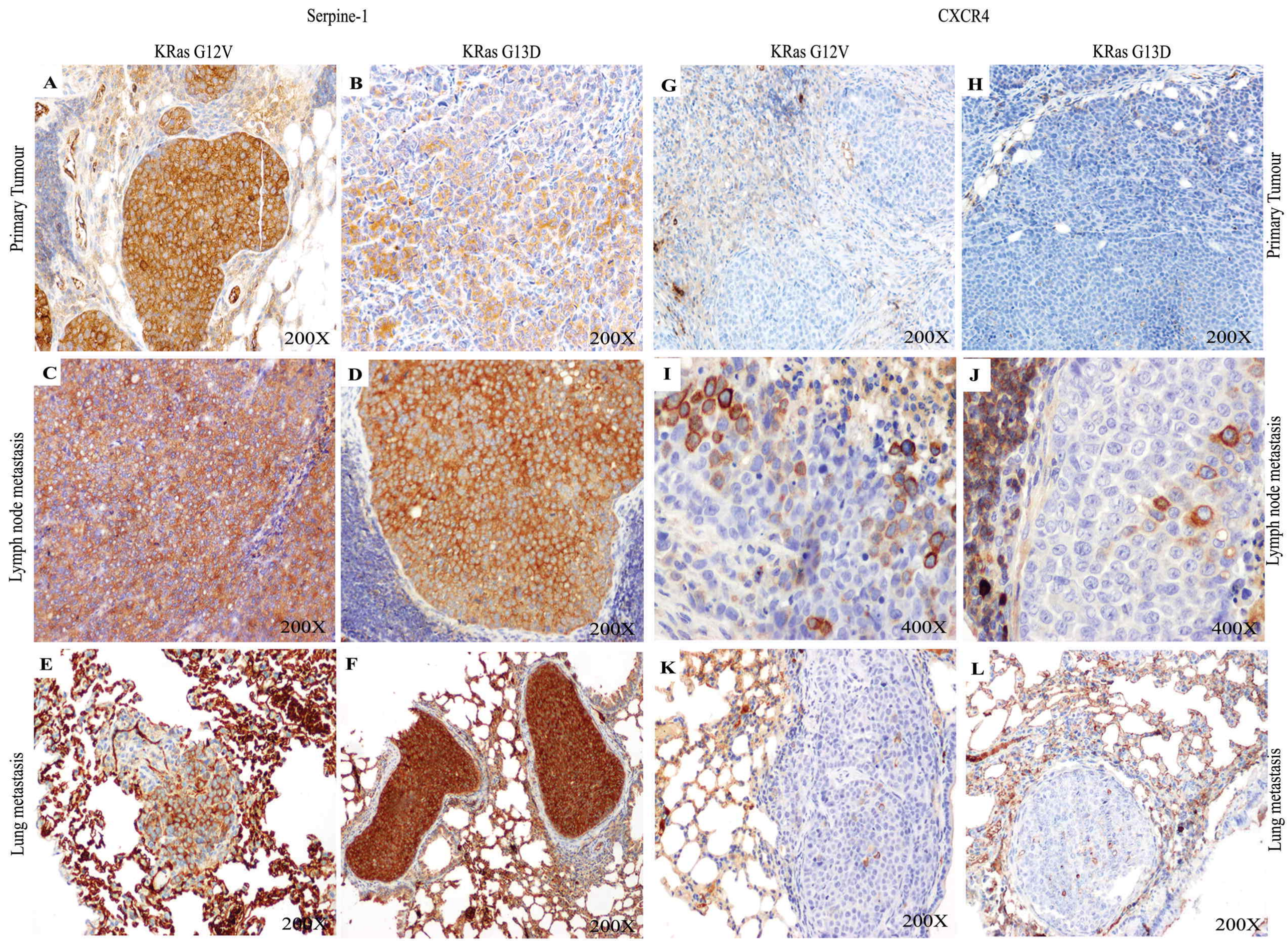
Serpine-1
CXCR4
KRas G12V
KRas G13D
KRas G12V
KRas G13D
Primary Tumour
Lymph node metastasis
Lung metastasis
A
B
G
H
C
D
I
J
E
F
K
L
200X
200X
200X
200X
200X
200X
400X
400X
200X
200X
200X
200X

Figure 5

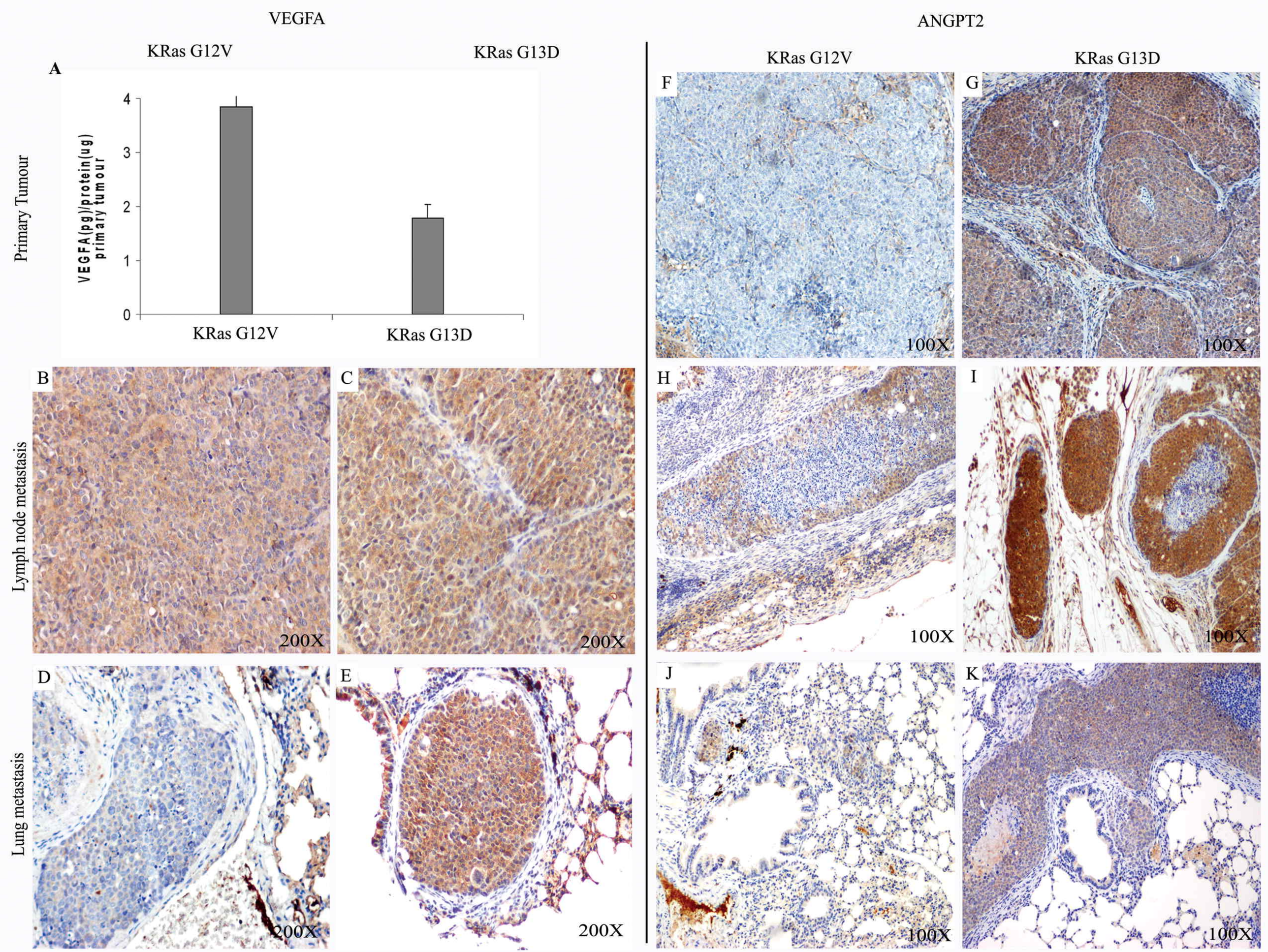
VEGFA
ANGPT2
KRas G12V
KRas G13D
A
VEGFA(pg)/protein(ug) primary tumour
4
3
2
1
0
KRas G12V
KRas G13D
Primary Tumour
Lymph node metastasis
Lung metastasis
B
C
D
E
F
G
H
I
J
K
200X
100X

Figure 6